Methods 61 (2013) 174–182

Contents lists available at SciVerse ScienceDirect

Methods

journal homepage: www.elsevier.com/locate/ymeth

# Methods for detection and analysis of apoptosis signaling in the *C. elegans* germline

Benjamin Lant, W. Brent Derry *

*Developmental & Stem Cell Biology, The Hospital for Sick Children, Toronto, ON, Canada M5G 1X8*
*Department of Molecular Genetics, University of Toronto, Toronto, ON, Canada M5S 1A8*

ARTICLE INFO

*Article history:*
Available online 2 May 2013

*Keywords:*
Germline
Stem cells
Apoptosis
*C. elegans*
DNA damage response
*In vivo* fluorescence markers

ABSTRACT

This review assesses current and emerging methods for the detection, and analysis of apoptosis in the *Caenorhabditis elegans* germline. The nematode worm *C. elegans* is highly tractable to genetic manipulation, making it an excellent model for elucidating mechanisms of apoptosis signaling in a multicellular setting. Here we profile the most efficacious fluorescent tools to visualize and quantify germline apoptosis. We focus specifically on the application of fluorescent markers to screen by RNAi for genes and pathways that regulate germline apoptosis under normal conditions or in response to genotoxic stress. We also present the limitations of these methods, and suggest complimentary techniques in order that researchers new to the field can comprehensively assess apoptosis phenotypes in the *C. elegans* germline.


## 1. Introduction

Sydney Brenner credited *Caenorhabditis elegans* as "Nature's gift to science" in his Nobel prize acceptance speech [1]. Indeed, this tiny transparent round worm has enabled the apoptosis field to emerge as one of the most exciting areas of biomedical research in the 21st century. During embryonic and larval stages of *C. elegans* development an invariant pattern of apoptosis occurs, where the majority of cells fated to die are in neural lineages [2,3]. In the hermaphrodite germline, two forms of apoptotic cell death occur: physiological and stress-induced [4–6]. In both cases apoptosis involves cellularization of the dying cell within the gonad syncytium, followed by phagocytosis by the surrounding gonadal sheath cells. The germline of a *C. elegans* hermaphrodite is organized as a symmetric bilateral tube connected at a central uterus in the middle of the body (Fig. 1). Each gonad arm is comprised of a mitotically proliferating population of stem cells at the distal end, which transition into the stages of meiosis I as they move proximally towards the uterus. As germ cells exit the pachytene stage of meiosis I they become competent to undergo physiological and stress-induced apoptosis [4,5].

The apoptotic death of most cells in *C. elegans* requires the core apoptosis signaling pathway, which is comprised of the BH3-only protein EGL-1, the anti-apoptotic Bcl2 orthologue CED-9, the apoptotic protease activation factor 1 (Apaf-1) orthologue CED-4, and the caspase CED-3 (Fig 2). Despite a thorough understanding of the core cell death machinery, there is much to be learned about the signals that govern a cell's decision to activate or repress the apoptotic program. For example, emerging evidence indicates that neighboring tissues play important roles in promoting both somatic and germline apoptosis. The engulfment proteins were first shown to cooperate with the core cell death pathway to promote apoptosis in the soma during development [11,12], suggesting that non-dying cells can influence the destiny of those fated to die. More recently, the gonadal sheath cell, which engulfs dying germ cells, has been shown to promote physiological germ cell death through Ephrin receptor signaling [13]. In response to genotoxic stress, the p53-like transcription factor is required in the dying cell to promote apoptosis by activating the expression of *egl-1* [14–16]. However, recent studies have shown that CEP-1 does not act alone. For example, the cytoskeletal binding protein KRI-1 is required in the soma to promote apoptosis in the germline by a mechanism that does not influence the transcriptional activity of CEP-1 [17]. In addition, the ASJ sensory neurons in the head of *C. elegans* hermaphrodites secrete a tyrosinase in response to DNA damage that is apparently transported to the germline where it can modulate the activity of CEP-1 [18]. The retinoblastoma orthologue has been shown to function in both the soma and germline to promote physiological germ cell apoptosis [19]. Forward and reverse genetics approaches have uncovered a number of other genes that regulate physiological and stress-induced germline apoptosis, but much work remains before these signaling modules can be assembled into a testable framework.

In this review, we focus on the use of established and emerging tools to study the regulation of apoptosis in the *C. elegans* germline. In particular, we highlight the power of reverse genetics methods in establishing and identifying apoptotic phenotypes, as well as

* Corresponding author at: Developmental & Stem Cell Biology, The Hospital for Sick Children, Toronto, ON, Canada M5G 1X8. Fax: +1 416 813 2212.
*E-mail addresses:* brent.derry@sickkids.ca, brent.derry@utoronto.ca (W.B. Derry).

1046-2023/$ - see front matter © 2013 Elsevier Inc. All rights reserved.
http://dx.doi.org/10.1016/j.ymeth.2013.04.022

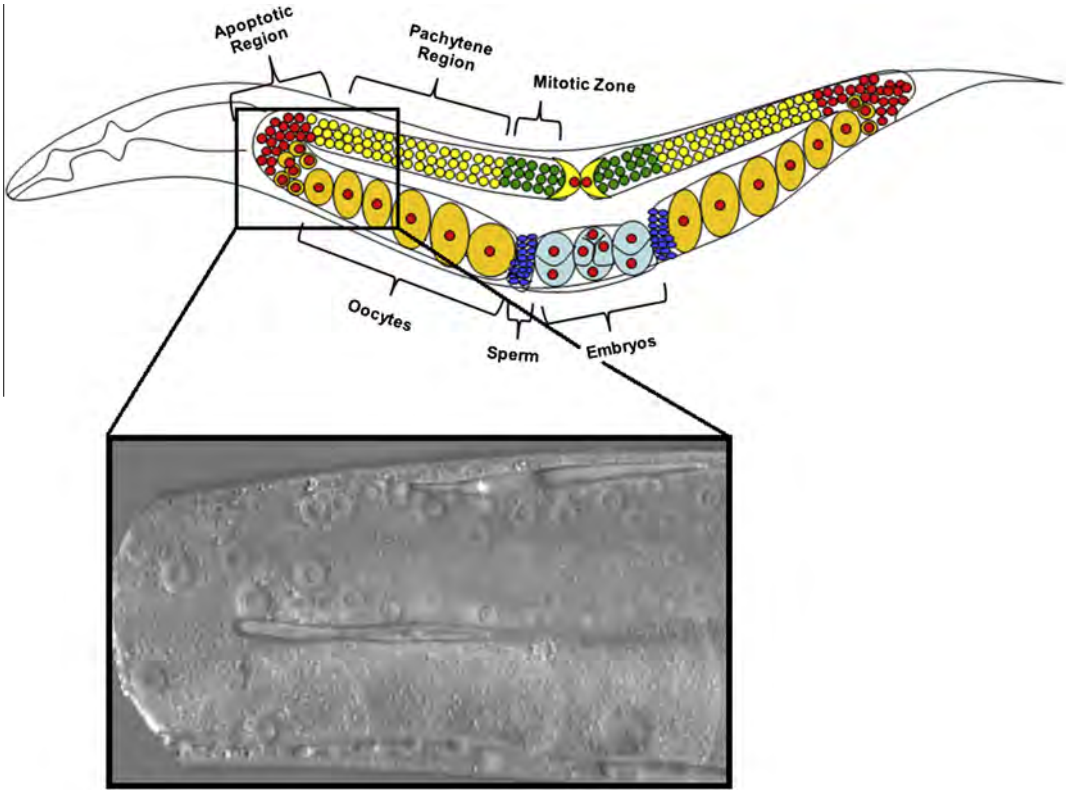


**Fig. 1.** The *C. elegans* germline. The top panel depicts a cartoon image of the two gonad arms. At the distal ends are the mitotically proliferating stem cells, which transition into meiosis I in the pachytene region. Apoptosis (physiological and stress-induced) occurs after the germ cells exit the pachytene stage of meiosis I, which is around the 'U-bend' region. After pachytene exit the first ~150 germ cells differentiate into sperm between the L4 and young adult stages of development. Oocytes are continuously produced from young adult stage to death of the hermaphrodite and fertilized oocytes undergo several rounds of embryonic cell division in the uterus before they are extruded from the vulva to the external environment. The lower panel shows a wild type (N2) young adult hermaphrodite gonad arm, where several pachytene stage nuclei and developing oocytes are visible (DIC optics, 630×).

current (and potential future) methods for imaging apoptosis in the germline of living animals. We have briefly outlined the most adaptable techniques for the efficient detection of apoptotic events, but for more comprehensive descriptions of standard protocols to analyze somatic and germline apoptosis in *C. elegans* we refer readers to the following recent reviews [20,21]. In seeking to fully exploit the advantages of *C. elegans* to understand the mechanisms of apoptosis, a myriad of mutant strains have been created. Primarily these mutations ablate function (partially or completely) of apoptosis genes, but there are also important 'gain of function' mutations available that offer added advantages in assigning pathway order. In terms of nomenclature, this review will henceforth refer to loss of function, null, and gain of function mutations as *lf*, *0*, and *gf*, respectively. If the reader is unfamiliar with basic *C. elegans* genetics we refer them to a valuable online resource called "Wormbook" [22]. Complimentary to the use of available mutant strains is the powerful application of gene knockdown technology using RNA interference (RNAi), which will be covered in depth later in this review.

## 2. Using mutant strains and RNAi to investigate germline apoptosis

The power of the nematode in apoptosis studies undoubtedly lies in its optical clarity and tractability to genetic manipulation. The extensive collection of available mutant strains and characterized RNAi libraries allow high throughput screens to be conducted with ease. Using these tools, phenotypic responses to apoptosis through a given family of proteins or signaling pathway can be assessed in a relatively short time-span, although it is necessary to be conscious of the effects of reduction versus elimination of function using RNAi or null alleles; and it is desirable to utilize both approaches (if possible) to confirm the effects of targeted genes that exhibit apoptosis phenotypes. Strains carrying mutations in key apoptosis genes and transgenic strains expressing fluorescent markers of apoptosis are summarized in Table 1 (Section 7). The RNAi reagents referenced further on in this review come from the Source BioScience LifeSciences RNAi bacterial feeding library, which covers 87% of the worm genome.

### *2.1. Physiological and damage induced apoptosis, and the core apoptotic machinery*

Pioneering genetic studies by Horvitz and colleagues led to the discovery and characterization of apoptosis genes that function in a linear signaling pathway to eliminate somatic cells during embryonic and larval development of *C. elegans*, which are conserved across phyla (Fig. 2) [23,24]. Subsequent studies initiated by Hengartner and colleagues showed that the core apoptotic pathway is also required for cell death in the hermaphrodite germline [4]. Activation of the core apoptosis pathway in almost all tissues of *C. elegans* involves tissue-specific transcription factors that regulate expression of the BH3-only gene *egl-1*. The p53-like gene *cep-1* is required for activating *egl-1* expression to promote stress-induced apoptosis in the germline (i.e., in response to DNA damaging agents), but *cep-1* is dispensable for both physiological germ cell apoptosis and developmental apoptosis in the soma [14,15]. Likewise, *egl-1* is required for stress-induced apoptosis but not physiological apoptosis in the germline [4,5]. Biochemical experiments suggest that the EGL-1 protein binds to and disables the

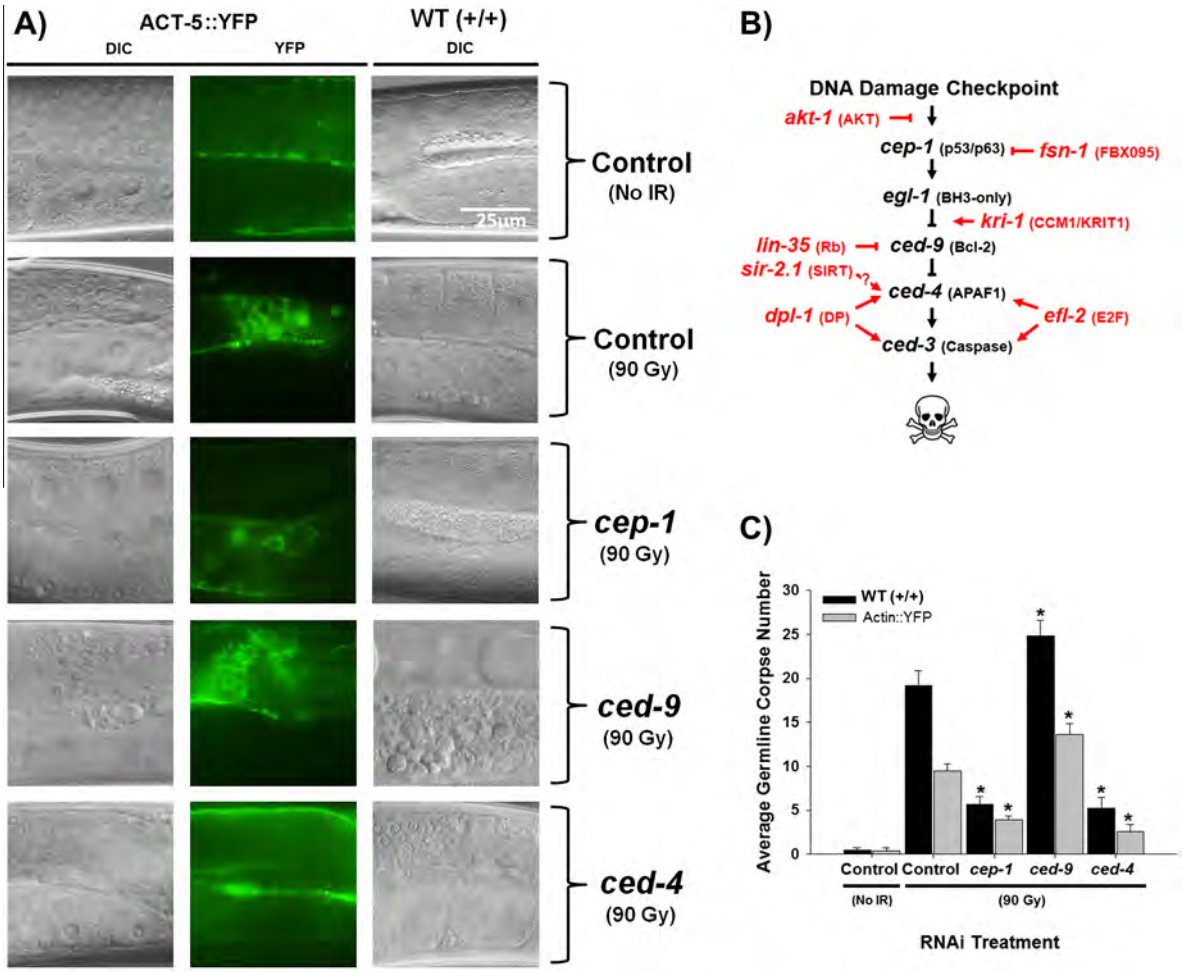


**Fig. 2.** Effect of apoptotic gene ablation by RNAi on germline apoptosis. Genes required for DNA damage-induced germline apoptosis (*cep-1*, *ced-9* and *ced-4*) were knocked down by RNAi to highlight their role in promoting apoptotic responses. In this example, images were taken 24 h after exposure of worms to 90 Gy of IR. (A) Comparison of strains expressing actin fused to YFP (ACT-5::YFP) in the gonadal sheath cells with wild-type (N2). White light and YFP channels were employed to visualize refractile germ cell corpses and actin bundles surrounding early stage apoptotic germ cells in the same field (left and middle panels) are compared with N2 late stage germ cell corpses (right panels). (B) Simplified depiction of the canonical DNA damage response apoptosis signaling pathway (human orthologues are indicated above *C. elegans* genes). (C) Mean corpse numbers for associated RNAi treatments; *cep-1*, *ced-9* and *ced-4* ablation induce expected effects on IR-induced apoptosis. * Indicates significantly different (at least $P < 0.05$; Student's *t*-test) from control (with IR).

**Table 1**
Strain information for visualizing and quantifying germline apoptosis.

| Strain | Genotype | References |
|---|---|---|
| Wild Type | N2 Bristol | [4,57] |
| WS2170 | *unc-119(ed3) III;* opIs110[$P_{lim-7}$::*YFP::ACT-5*; *unc-119(+)*] IV | [38] |
| MD701 | bcIs39[$P_{lim-7}$::*CED-1*::GFP; *lin-15*(+)] V | [36] |
| CB3203 | *ced-1(e1735)* I | [4,58] |
| MT1522 | *ced-3(n717)* IV | [4,59] |
| MT2547 | *ced-4(n1162)* III | [60] |
| MT3970 | *mab-5(mu114) ced-9(n1653)* III | [61] |
| VC172 | *cep-1(gk138)* I | [62] |
| MT8735 | *egl-1(n1084n3082)* V | [7] |
| OD95 | *unc-119(ed3)* III; ltIs37[$P_{pie-1}$::mCherry::HIS-58; *unc-119(+)]* IV; ltIs38[$P_{pie-1}$::GFP::PH(PLC1delta1); *unc-119(+)*] | [51] |
| SD551 | *let-60(ga89)* IV | [41,63] |
| MT10430 | *lin-35(n745)* I | [19,64] |
| SD378 | *mpk-1* (ga117)/*dpy-17(e164)*/ *unc-79(e1068)* III | [41,65] |
| WS2972 | *gla-3(op216)* I | [41] |
| NL2098 | *rrf-1(pk1417)* I | [17,54,56] |
| NL2550 | *ppw-1(pk2505)* I | [17,55] |

Bcl2-like protein CED-9 from inhibiting CED-4, which in turn, is required to activate the proteolytic caspase CED-3 [7–10,25–27]. However, the long held notion that CED-4 resides at the mitochondria in a molecular complex with CED-9 has been challenged by recent observations disputing their colocalization [28]. This suggests additional factors might be required in mediation of the core apoptotic signaling pathway in this organism. Forward genetics have not as yet uncovered potential candidate genes that would settle this debate, with the possible exception of the mitochondrial apoptosis-inducing factor WHA-1

or the EndoG homologue CPS-6 [29,30], but more work is undoubtedly required.

The CED-3 caspase targets a number of protein substrates, whose cleavage collectively leads to dismantling of the doomed cell by mechanisms that are presently not well understood [31]. Initially through global proteomics, Taylor et al. found that approximately 3% of the *C. elegans* proteome is targeted by CED-3 for proteolysis [31]. Subsequently, Crawford et al. have identified 50 CED-3 cleavage sites, through an *in vitro* N-terminal labeling protocol with a CED-3 preparation [32]. Although there is varying conservation in exact cleavage sites between human and nematode proteins, there is a high conservation in terms of functional pathways and specific protein targets [32]. Conserved human targets include structural proteins, such as actin and tubulin, as well as Rho signaling molecules [32]. Given that these downstream targets of CED-3 likely collaborate in the early and late stages of apoptotic cell death, ablation of these proteins alone may not give detectable apoptotic phenotypes using conventional methods. Thus, it will likely be necessary to ablate multiple proteins in combination to uncover robust apoptosis phenotypes involving CED-3 substrates. With this in mind, reagents allowing for more sensitive dissection of the early and late stages of apoptosis will be helpful in teasing apart the roles of individual genes that affect specific stages of this signaling cascade.

### 2.2. Corpse engulfment as a marker of apoptosis

In terms of markers of the apoptotic process, alongside the core apoptosis signaling proteins are proteins involved in cell corpse engulfment. Typically engulfment is swift and carried out by neighboring cells through phagocytosis. The engulfing body (phagosome) is formed when the neighboring cell recognizes "eat-me" signals on the surfaces of dying cells. The exposure of phosphatidylserine (PS) on the outer leaflet of the plasma membrane, causing phospholipid asymmetry, is an engulfment signal conserved across phylogeny [33,34]. Engulfment itself is a highly orchestrated multi-step process that involves substantial rearrangements of the actin cytoskeleton within the engulfing cell as it surrounds the dying cell [35]. Amongst the primary engulfment proteins, the transmembrane protein CED-1 is critical to PS binding and mediation of corpse engulfment. CED-1 is commonly used as an apoptotic marker when fused to the green fluorescent protein (GFP) [36].

### 2.3. Using core apoptotic machinery, and actin, to stage and assess DNA damage induced apoptosis

Given that the core apoptosis signaling molecules exhibit robust knockdown phenotypes in the *C. elegans* germline, they should be used as relative controls when screening for apoptosis regulators by reverse genetics methods. Fig. 2a shows the effects of knocking down *cep-1*, *ced-4* or *ced-9* by RNAi on DNA damage-induced germline apoptosis; in this case ionizing radiation (IR) was used. Germline apoptosis was assessed using both the wild type strain (as per *C. elegans* convention, we henceforth refer to the wild type strain as N2 Bristol – see Table 1 for details) and a transgenic strain expressing actin fused to yellow fluorescent protein (YFP) in the gonadal sheath cells (ACT-5::YFP); previously shown to highlight apoptotic cells [37,38]. In the early stages of apoptosis ACT-5::YFP halos surround cells fated to die, which are detectable by differential interference contrast (DIC) optics as refractile 'button-like' corpses at later stages of apoptosis (Fig. 2a). The images, taken at 630x magnification indicate the efficacy of ACT-5::YFP corpse labeling, which responds to the RNAi treatments as expected, even though some are too early to be detected by DIC optics. It is important to note that Fig. 2a shows both white light and fluorescence views of the same plane (panels on left side) to illustrate the YFP signal in early-stages of apoptosis, where corpses are not obvious by morphological criteria. Late-stage corpses are shown in N2 germlines (panels on right side) under the same conditions for comparison. Fig. 2c subsequently shows relative germ cell corpse numbers in response to IR and ablation of various apoptosis genes by RNAi. The trends of corpse numbers in response to either IR or RNAi treatment (or both) are consistent with previous findings. Inhibition of either *cep-1* or *ced-4* confers resistance to apoptosis, whereas inhibiting *ced-9* causes massive levels of apoptosis in the germline that are similar in the absence or presence of genotoxic stress (i.e. [14,15,39,40]).

### 2.4. Using mutant strains to delineate physiological from damage induced apoptotic phenotypes

Because physiological and stress-induced germline apoptosis involve distinct regulatory inputs it is important to use appropriate controls to differentiate genes that regulate these pathways. For example, a gene identified in a high throughput screen that causes increased corpse numbers might function by perturbing the core apoptosis pathway, mitogen activated protein kinase (MAPK) signaling, or by activating the DNA damage response (Fig. 2b). For example, inactivation of the retinoblastoma (RB) gene *lin-35* and members of the RB complex result in reduced levels of physiological and DNA damage-induced germline apoptosis because they affect transcription of the core apoptosis genes *ced-9*, *ced-3* and *ced-4* [19]. Ablation of the germline apoptosis abnormal *gla-3* gene results in increased physiological germline apoptosis by activating MAPK signaling [41]. Thus, quantitative real-time PCR of core apoptosis genes and antibody staining to the phosphorylated (activated) extracellular signal-regulated kinase (ERK) homologue MPK-1 are important molecular markers to delineate how various proteins control the apoptosis program [16,19,20,41–43]. Since both *cep-1* and *egl-1* are required for DNA damage-induced apoptosis, but dispensable for physiological germline apoptosis, strains carrying mutations in these genes can be used to perform genetic epistasis analysis in order to determine if a candidate gene functions through the physiological or stress-induced apoptosis signaling pathways. Similarly, genes that reduce germline apoptosis when ablated can be examined in the context of *gla-3* and *ced-9* loss-of-function alleles to order them relative to upstream and core apoptosis genes.

While the above gene targets all have direct roles in either execution of germ cell death or corpse degradation, members of the MAPK pathway such as *let-60*/RAS upstream of *mpk-1* and pachytene arrest/oogenesis signals, are germline apoptosis regulators as well [4,43,44]. However, in some cases alteration of apoptosis could be the consequence of indirect effects on meiotic progression. Thus, distinguishing between genes that prevent pachytene exit versus those which specifically inhibit physiological apoptosis is critical since MAPK signaling controls both of these processes. Hence, immunostaining of phosphorylated MPK-1 can be used to assess whether meiotic germ cells in a given mutant strain are competent to undergo apoptosis [43]. For example, down regulation of the insulin signaling pathway (i.e. *daf-2(lf)* mutants) reduces phosphorylated MPK-1 to levels that confer resistance to DNA damage-induced germline apoptosis but does not affect meiotic progression[45]. The question of whether the apoptosome is functional in a given mutant strain, such as *daf-2(lf)*, can be easily assessed by manipulating the dosage of *ced-9*, which when knocked out causes massive apoptosis in DNA damage checkpoint mutants or when other pro-apoptotic signaling pathways are compromised [17,19,39,46]. In *mpk-1* mutants, ablation of *ced-9* cannot activate apoptosis since the germ cells do not exit the pachytene stage of meiosis and are therefore not competent to undergo apoptosis [41]. However, ablation of *ced-9* in *daf-2(lf)*

mutants restores apoptosis to normal levels, indicating that the apoptosome is functional but signals to activate it are blocked [45]. Should you choose to immunostain for markers such as phosphorylated MPK-1, it is beneficial to co-stain with 4',6-diamidino-2-phenylindole (DAPI), a DNA intercalating dye. This allows you to accurately compare corpse numbers with total germ cell numbers to ascertain whether there is a legitimate effect on apoptosis or altered germline proliferation. This is particularly important for analyzing mutant strains that are resistant to apoptosis but also have smaller germlines.

### 2.5. Monitoring engulfment rates to reduce false positive apoptotic signals

As with changes in *ced-9* dosage, small alterations in corpse engulfment rate can have significant effects on quantification of corpse numbers. The germline is constantly proliferating, where approximately 50% of germ cells produced undergo apoptosis and get engulfed at a constant rate [4]. It is therefore important to differentiate between elevated levels of apoptosis and perceived increases due to corpses that do not get efficiently engulfed. This can be easily achieved by monitoring the time between corpse appearance and engulfment in living animals (i.e., [42]). For example, it is possible to analyze engulfment rate (and indeed engulfment defects) by following the fate of a single corpse over a set period of time. Standard corpse budding, maturation and engulfment completes within 30–40 min [4], hence aligning a sequential series of pictures taken over short intervals (2–5 min) can provide a detailed analysis of the morphological features of cell death and engulfment rate in a given mutant strain, after gene knockdown, or in response to various stresses. In addition, apoptosis counts can be conducted in engulfment defective mutants, such as *ced-1* or *ced-5*, to increase the sensitivity of detecting modest changes in apoptosis [33,39].

### 2.6. Statistical quantification of germline apoptosis

The statistical methods for analyzing changes in apoptosis should also be carefully considered. For example, DNA damage causes a substantial increase in corpse numbers that generally follow a normal (bell curve) distribution, which can be analyzed using the Student's *t*-test. On the other hand, levels of physiological apoptosis generally follow Poisson distribution, which cannot be compared with data that follows normal distribution using the *t*-test. We recommend using the Mann–Whitney *U* test because this method does not assume the data sets follow normal distributions. Therefore, caution should be exercised when applying various statistical methods to determine the significance of changes in germline apoptosis.

## 3. DNA degradation and germline staining

While the pathway targets of apoptosis and engulfment are well documented, various detection methods have been adapted significantly over the years; beginning with the concept of using DNA degradation (a conserved apoptotic response) as a potential marker for indicators and dyes. However, degradation of DNA is difficult to visualize *in vivo* unless worms are fixed and stained with a reagent that specifically labels degraded DNA, such as terminal deoxynucleotidal transferase (TdT)-mediated dUTP nick end labeling (TUNEL) [47] or DAPI. As an alternative to TUNEL and DAPI, apoptotic nuclei can be easily visualized using a number of staining procedures that do not rely on fixation. Vital dyes such as acridine orange (AO) and SYTO-12 facilitate quantification of apoptotic nuclei in the germline of *C. elegans* hermaphrodites by simply soaking living animals in a solution of the dye or feeding them bacteria that has been soaked in the dye [4,14,48]. These membrane permeable dyes use the low pH of cells (during apoptosis) to intercalate double-stranded nucleic acids and subsequently emit fluorescence.

One drawback to the use of AO and SYTO-12 in *C. elegans* is that these dyes do not label apoptotic nuclei in engulfment-defective mutants [6,49]. Thus, it is important to take into consideration the genetic background of the strain when using fluorescent dyes, and use DIC microscopy to confirm observations with these reagents (Fig. 3a). Another drawback to the use of dyes is high background fluorescence, which requires that worms be placed on dye-free bacteria for approximately 2–3 h in order to clear dye from the intestine. For best results excess dye should be cleared to visualize apoptotic nuclei in living worms. The main advantages of using AO or SYTO-12 are that their bright signals enable visualization of corpses using lower power microscopes, and the simplicity of their application. For example, AO and SYTO-12 are ideal reagents for high throughput apoptosis screens using a fluorescence dissecting microscope (Fig. 3b) [48]. Compared with the time required to pick and mount worms on a slide, this method is one of the most efficient. Fig. 3a shows at both 10× and 50× magnification, low and high apoptosis levels can be quite easily discerned using AO staining. This method of detection is well suited for carrying out systematic RNAi screens to identify genes that regulate apoptosis under normal growth conditions and in response to stress (as indicated by IR treatment in Fig. 3a). The benefits of this are clear for screens, where handling and procedural steps are minimized and the worms remain viable. As shown in Fig. 4, AO stains corpses that are also evident by their refractile morphology under DIC optics. Since AO (or SYTO-12) is selectively retained in apoptotic cells these dyes ensure that these bodies are indeed apoptotic and not morphological features that resemble apoptotic corpses. Another advantage of combining vital dyes with DIC optics is that they can help differentiate between mid-stage (Fig. 4 (1)), mid to late-stage (Fig. 4 (2)) and late stage (Fig. 4 (3)) corpses. Perhaps the most useful aspect of their combined use is in training the inexperienced to recognize the morphological features of apoptotic corpses in the germline. Like most anatomical assays it takes a lot of practice and patience to become adept at scoring apoptotic corpses using DIC microscopy.

## 4. Using fluorescently labeled proteins

The use of fluorescently tagged proteins to visualize apoptosis in the germline is well documented, primarily through the use of the CED-1::GFP fusion protein, which labels corpses poised for (or undergoing) engulfment *in vivo*[36]. Germ cell corpses, surrounded by gonadal sheath cells, fail to get properly engulfed in the absence of CED-1 (i.e., in *ced-1* (*e1735*) mutants) [36]. While use of these mutants is advantageous for determining if subtle differences in corpse numbers are significant, accumulation of un-engulfed corpses in the distal germline can be difficult to quantify; compounded with the observation that some CED-1::GFP labeled cells fail to complete apoptosis [20]. As an alternative reagent, expression of ACT-5::YFP in the gonad sheath cells provides a highly specific marker for early stage corpses [37,38]. Like CED-1 protein, actin cables form dense halo's around cell corpses but in our experience it is easier to distinguish individual corpses using the ACT-5::YFP reporter. While both CED-1 and actin are required for the engulfment process (and both produce halos around cells targeted for apoptosis), there is no evidence that CED-1 and actin co-localize and as such have a relative functional separation [38]. Hence the use of ACT-5::YFP becomes a viable alternative to

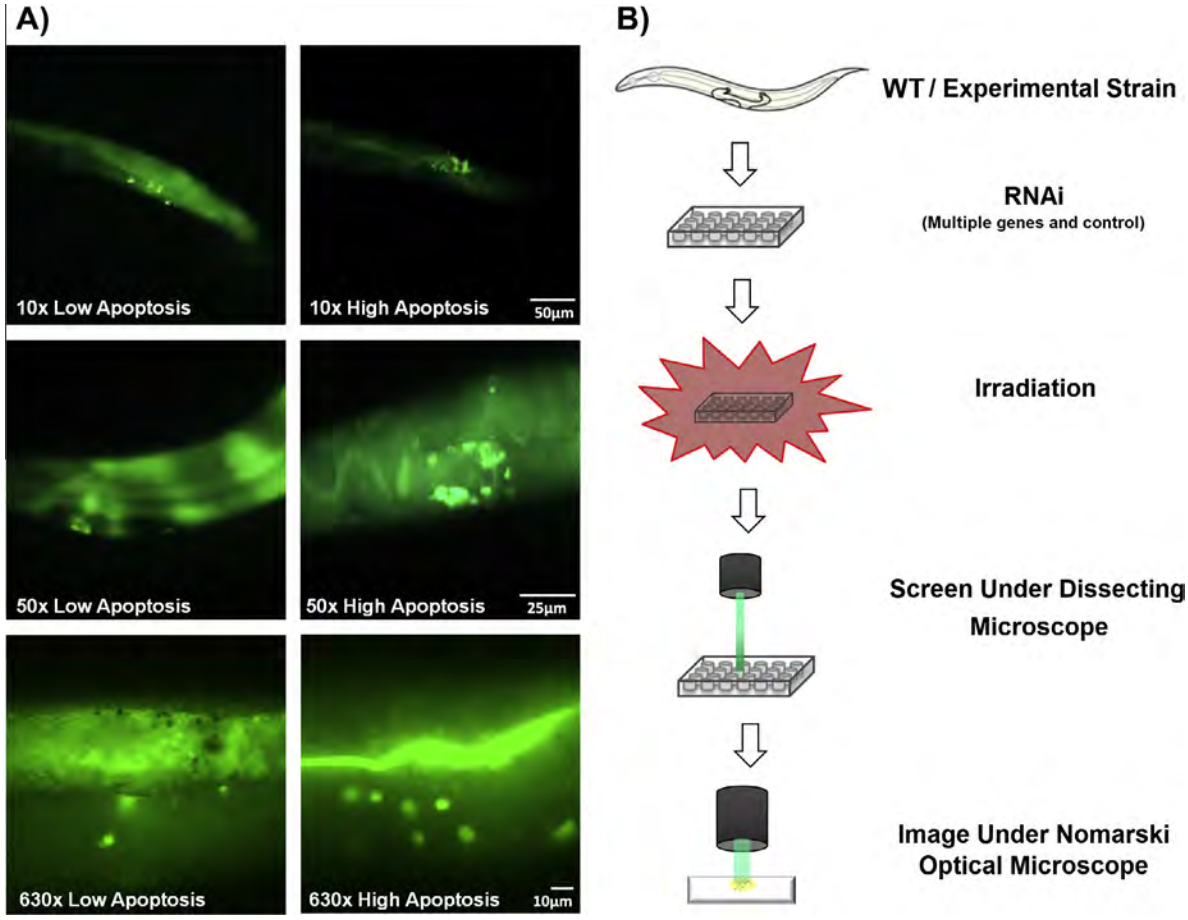


**Fig. 3.** Methods for high throughput screening of *C. elegans* for germline apoptosis genes. (A) Comparison of apoptosis visualization between low resolution dissecting microscope and high resolution DIC optics. Germline apoptosis detected by Acridine Orange staining; Left side panels indicate low level apoptosis, right side panels indicate high level apoptosis (induced by 90 Gy IR). From the top; 10× magnification, 50× magnification (both captured with dissecting microscope) and 630× magnification. Quantification of apoptosis is possible, but best precision is achieved at high resolution using DIC optics. (B) Schematic for germline apoptosis screening strategy by RNAi.

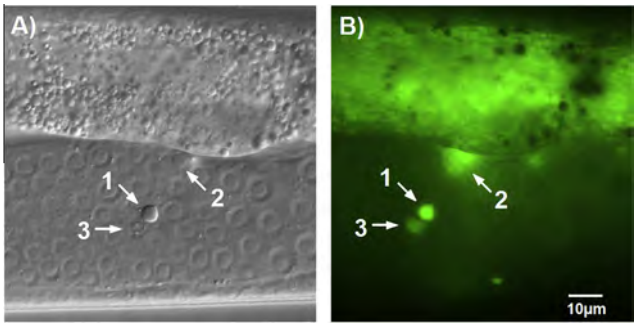


**Fig. 4.** Visualization of germline corpses at high resolution by (A) white light (DIC optics, 630× magnification) and (B) in the GFP channel using Acridine Orange to detect corpses. Germ cell corpses at mid (1) mid-late (2) and late (3) stages are shown in a single plane of the *C. elegans* germline.

CED-1::GFP, without the apparent caveats (as of yet). It should be noted that actin::YFP is specific to detection of early to mid stages of apoptosis, as there was little overlap between ACT-5::YFP halos and either Hoechst 33342 or SYTO 41 staining; markers of late stage apoptosis [38]. In this context, ACT-5::YFP can also be used to predict where corpses will arise (visualized later as refractile bodies by DIC). Using ACT-5::YFP as an alternative marker of germline apoptosis (Fig. 2A,C) we find that it provides a crisp fluorescent signal more representative of steady-state (physiological) apoptosis that can be viewed using low and high magnification optics. Although expression of ACT-5::YFP in the gonadal sheath cells confers some resistance to germline apoptosis, there is an equivalent relative response to IR in comparison to N2 worms (Fig. 2C). For use in high throughput RNAi screens, we also find the lower background of ACT-5::YFP (compared to CED-1::GFP) to be more efficacious (Lant and Derry, unpublished).

## 5. Future prospects

As the apoptosis field develops, increasing numbers of useful transgenic strains are becoming available, allowing for greater analysis of stage-specific events in the apoptotic cascade. One recently constructed strain expresses the fluorescently-tagged fusion protein TTR-52::mCHERRY::FLAG. TTR-52 is a novel secretory protein that clusters around apoptotic cells by recognizing surface exposed PS [50]. TTR-52::mCHERRY::FLAG labels apoptotic germ cells on the surface of dissected gonads, which increases in response to RNAi knockdown of *gla-3* as well as a mutation in *tat-1* (an aminophospholipid translocase that mediates PS asymmetry) [50]. Another recent addition to the germline toolkit is a strain expressing mCherry tagged to the histone protein HIS-58 and GFP that targets the plasma membrane (Table 1) surrounding the germ cell nuclei (rachis). These markers, originally used to measure cortical contractility [51] were recently used in a screen for germline phenotypes, including altered apoptosis (detected by condensed HIS-58::mCherry chromatin) [52]. We have confirmed

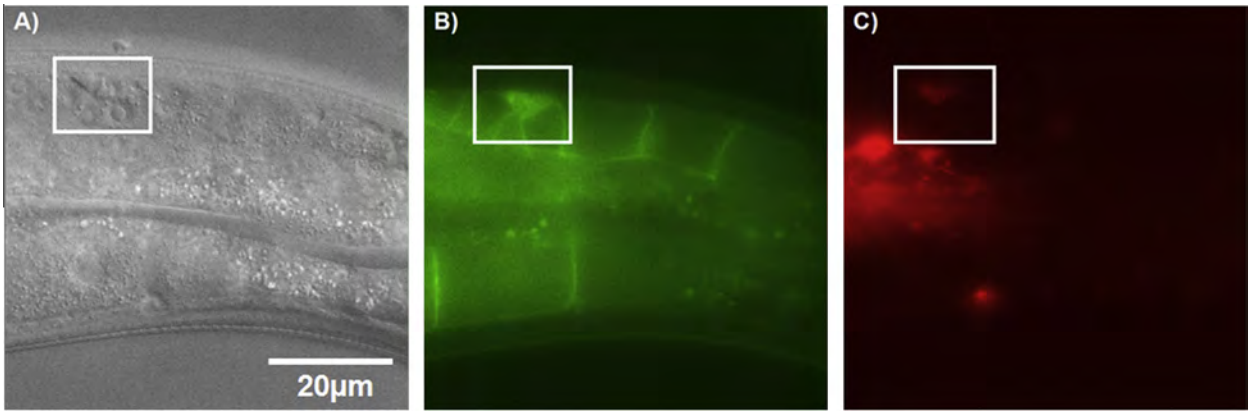


**Fig. 5.** Multichannel analysis of apoptosis detection using a strain that expresses mCherry fused to the histone protein HIS-58 (red) and the PH domain of the phospholipase C delta 1 protein (green). OD95 strain genotype: *ltIs37* [*pie-1p*::mCherry::HIS-58 + *unc-119(+)*] IV; *ltIs38* [pAA1; *pie-1p*::GFP::PH(PLC1delta1) + *unc-119(+)*]. Sections (A), (B) and (C) show white light (DIC optics), GFP, and RFP channels respectively; boxing indicates region where germ cell corpses are visible.

that this strain not only has potential for detecting condensed DNA, but suggest combining with the ACT-5::YFP to serve as a highly sensitive tool for imaging multiple phases (early – actin halos, late – histone condensation) of apoptosis concurrently. As shown in Fig. 5, the three channels (White, Green and Red), all exhibit the hallmark features of apoptosis; corpse budding (5A), membrane alteration (5B) and DNA condensation (5C), respectively. This strain is also particularly useful through its ability to mark all germ cells, which can be used to normalize corpse counts to total germ cells under any experimental condition. This is important because in some cases changes in corpse numbers might simply reflect altered germline proliferation. We therefore recommend comparing germ cell numbers in the pachytene region with corpse numbers when effects of gene knockdown on apoptosis are subtle.

When considering screening under low magnification, 50x is capable of detecting both ACT-5::YFP ringed corpses, as well as mCherry::HIS-58 labeled DNA condensation [52]. Although in comparison to AO stained cells the mCherry signal is significantly weaker. The use of fluorescently tagged proteins, however, could be seen as more efficacious in terms of screening than the AO procedure by removing the necessity for AO handling and the subsequent background optimization. Here the limitation is magnification and detection technology. Resolution improves with magnification (best resolution is at 630 or 1000x) which increases the usefulness of fluorescent tags over dye staining procedures. We must caution that strains expressing mCherry::Histone and GFP::PH in the germline appear largely resistant to DNA damage-induced apoptosis (averaging ~2 corpses with 90 Gy IR), but we confirm that germ cells are capable of undergoing apoptosis when *ced-9* is knocked down (Lant & Derry, unpublished). Similarly, ACT-5::YFP corpse numbers (induced by IR; Fig. 2c) are slightly below N2 levels for reasons currently unknown, but the strain responds equivalently (with regards to N2) when core apoptosis genes are knocked down by RNAi. More work using the appropriate controls will be necessary to ensure that these reagents are suitable for identifying apoptosis regulators by screening.

## 6. Protocols

### 6.1. Cultivation of C. elegans strains

**We refer readers to** the "Maintenance of *C. elegans*" chapter of Wormbook (http://www.wormbook.org/chapters/www_strainmaintain/strainmaintain.html) for detailed protocols describing cultivation, maintenance, and archiving of *C. elegans* strains [53].

### 6.2. RNAi protocol

- Using the *C. elegans* RNAi feeding library from Source BioScience LifeSciences (http://www.lifesciences.sourcebioscience.com/clone-products/mirna–rnai-resources/c-elegans-rnai-library/celegans-database.aspx) select negative controls (such as an empty RNAi plasmid in the HT115 bacterial strain), and positive controls such as *cep-1*, *ced-4* and *ced-9* RNAi expressing strains.
- Streak target RNAi out on LB + ampicillin (AMP) + tetracycline (TET) plates (refer to Ref. [53] for recipes), and grow for 24 h at 37 °C.
- Select single colonies and transfer to 4 ml liquid cultures (LB + AMP + TET; see below). Grow overnight on a shaker at 37 °C.
- Following this, add 20 µl 0.1 M IPTG to the culture and incubate for an additional 4 h at 37 °C.
- Aliquot 70–100 µl of the liquid culture on RNAi media plates (see below).
- Allow the bacterial lawn to grow overnight at room temperature (or 37 °C for thicker lawns) with lids on the plates to prevent contamination.
- Transfer approximately 25 N2 worms staged at the L1 larval stage to their respective plates and allow them to grow until the young adult stage; prior to irradiation. *If the gene in question is essential we advise placing worms on at a later stage of development, such as L3 or L4, in order to knock down the gene without causing severe effects on development.*

### 6.3. Ablation of genes by RNAi in the soma versus germine

In recent years both physiological and stress-induced germline apoptosis have been shown to require input from various somatic tissues [11–13,17–19]. Therefore, when assessing a candidate apoptosis gene it is important to determine the site of action. Strains are available that selectively abolish the effect of feeding RNAi in the soma or germline. For example, *rrf-1(pk1417)* mutants are resistant to RNAi in the soma whereas *ppw-1(pk2505)* mutants are resistant to RNAi in the germline [54,55]. Some genes also cause severe morphological defects when ablated in the soma, which can obstruct visualization of the germline. Thus, ablating genes in *rrf-1(lf)* mutants can help determine whether the effect on germline apoptosis is cell-nonautonomous or prevent pleiotropic phenotypes that might complicate visualization of germ cell corpses. However, a recent study reported that some somatic tissues remain sensitive to RNAi in *rrf-1(lf)* mutants [56]. Thus, we recommend that users exercise caution when using these mutants or verify phenotypes in other strains defective in RNAi in the soma.

### 6.4. Irradiation protocol

- Pick 25–40 worms from a plate at the fourth larval stage (L4) one day prior to irradiation. The following day, with worms now at the young adult stage, expose them to a dose of IR (0–120 Gy).
- Twenty-four hours after irradiation, observe worms by microscopy for abnormal levels of germline corpses using fluorescent dyes to label apoptotic nuclei or transgenic strains expressing fluorescent markers of early and late stages of apoptotic cell death.
- In both cases, germlines can be pre-screened using low-resolution fluorescence dissecting microscopes or high-resolution DIC microscopes equipped with fluorescence optics. The best resolution of morphological features at early and late stages of apoptosis is achieved at 630× (using a 63× oil immersion lens). If you require quantitative analysis of apoptosis, DIC optics are generally the most reliable.

### 6.5. AO staining protocol

- Place adult stage worms on a 35 mm bacterial plate containing the RNAi bacterial strain of interest approximately 20 h after they have been irradiated.
- Dilute Acridine Orange (AO; Molecular Probes Inc. A3568) from stock to 10 mg/ml; 7.5 μl AO in 1 ml of M9 buffer (see below).
- Carefully pipette 200 μl of diluted AO onto the surface of the bacterial lawn containing the irradiated worms (rotate the plate to allow absorption across the whole lawn).
- Store the AO-containing plates in the dark for 1hr, then transfer worms to a fresh plate containing the same RNAi expressing bacterial strain and incubate at room temperature in the dark for another 3 h to remove (de-stain) the excess AO form their intestines.
- Vizualize the worms to check for background. At this point, you can check the level of staining on a fluorescent dissecting microscope prior to slide mounting, to assess whether you need to de-stain more and reduce the background.

### 6.6. Visualization of apoptotic corpses in vivo

Following RNAi/IR treatments, worms can be viewed on the bacterial plate using a fluorescence dissecting microscope or mounted on a slide and viewed using DIC optics.

- To prepare samples for DIC microscopy, sandwich a thin 4% (w/v) agar pad between two slides to prevent the coverslip from crushing the worms. Please refer to the review by Craig et al. (Ref. [20]) for a detailed description of this protocol.
- Pick irradiated/RNAi treated worms from their plates into a 2.5 μl drop of 20 mM tetramisole (to anesthetize the worms) on the surface of a thin agar pad.
- Carefully drag the worms to the edge of the tetramisole drop in the middle of the agar pad, then place a coverslip over the worms sandwiching them between the coverslip and agar pad on the slide. Be careful to avoid trapping air bubbles against the bodies of the mounted worms as this will distort the light and make visualization of corpses difficult.
- Add about 10 μl of 20 mM tetramisole under the edge of the coverslip so the worms are adequately hydrated (but not enough to lift the coverslip off the pad).

We recommend that apoptotic corpses be visualized/quantified within one hour of mounting worms onto slides since germlines tend to degrade after a longer period of time in tetramisole. All images shown were created using a 630× oil immersion lens on a Leica DMRA compound microscope.

High throughput screening by fluorescence dissecting microscopy is markedly quicker than analysis of corpse numbers using high resolution DIC optics, but sacrifices some precision as a result. To simplify corpse analysis by AO staining using a fluorescence dissecting microscope, worms can be anesthetised in a drop of 20 mM tetramisole prior to visualizing. This is particularly important if you wish to capture images of AO-stained corpses since the movement of worms can blur images captured by the camera. AO stained corpses are indicated by round, intensely green filled bodies found in the bend region of the distal germline. Be careful not to mistake germ cell corpses with spermatocytes closer to the uterus, which can also take up AO and SYTO-12 dyes. ACT-5::YFP corpses are indicated by circular outlines of early stage corpses, whereas mCherry::HIS-58 apoptotic bodies are condensed red structures (condensed DNA) denoting later stages of apoptosis. In all cases, fluorescent apoptotic 'bodies' should be confirmed at high resolution using DIC optics.

## 7. Strains recommended

See Table 1.

## 8. Recipes

**NGM media(1 L)**; 3 g NaCl, 2.5 g Peptone, 20 g Agar and $dH_2O$ up to 1 L volume. Autoclave for 30 min, and let cool for 1 h at 55 °C (water bath). Following this, add 1 ml cholesterol (5 mg/ml), 1 ml $CaCl_2$ (1 M), 1 ml $MgSO_4$ (1 M) and 25 ml $KPO_4$ (1 M, pH 6).

**RNAi plates**; Add 3.12 ml IPTG (0.8 M) and 500 μl carbenicillin (50 mg/ml) to 1 L NGM media.

**LB + Amp + Tet media(1 L)**; 10 g Tryptone, 5 g Yeast extract, 10 g NaCl, 15 g Agar and $dH_2O$ up to 1 L volume. Autoclave for 30 min, and let cool for 1 h at 55 °C (water bath). Following this, add 2 ml Ampicillin (50 mg/ml) and 2 ml tetracycline (5 mg/ml).

**M9 Buffer (1L)**; 3 g $KH_2PO_4$, 6 g $Na_2HPO_4$, 5 g NaCl and $dH_2O$ up to 1L volume. Autoclave for 20 min and add 1 ml $MgSO_4$ (1 M).

## Acknowledgement

This work was funded by an operating grant from the Canadian Institutes for Health Research (MOP79495) to WBD a fellowship from the EIRR21st Radiation Medicine Research Program to BL.

## References

[1] S. Brenner, Biosci. Rep. 23 (5–6) (2003) 225–237.
[2] J.E. Sulston, H.R. Horvitz, Dev. Biol. 56 (1) (1977) 110–156.
[3] J.E. Sulston et al., Dev. Biol. 100 (1) (1983) 64–119.
[4] T.L. Gumienny et al., Development 126 (5) (1999) 1011–1022.
[5] A. Gartner et al., Mol. Cell 5 (3) (2000) 435–443.
[6] A. Gartner, P.R. Boag, T.K. Blackwell, WormBook (2008) 1–20.
[7] B. Conradt, H.R. Horvitz, Cell 93 (4) (1998) 519–529.
[8] L. del Peso, V.M. González, G. Núñez, J. Biol. Chem. 273 (50) (1998) 33495–33500.
[9] B. Conradt, H.R. Horvitz, Cell 98 (3) (1999) 317–327.
[10] L. del Peso et al., J. Biol. Chem. 275 (35) (2000) 27205–27211.
[11] D.J. Hoeppner, M.O. Hengartner, R. Schnabel, Nature 412 (6843) (2001) 202–206.
[12] P.W. Reddien, S. Cameron, H.R. Horvitz, Nature 412 (6843) (2001) 198–202.
[13] X. Li et al., Cell Death Differ. 19 (6) (2012) 1080–1089.
[14] W.B. Derry, A.P. Putzke, J.H. Rothman, Science 294 (5542) (2001) 591–595.
[15] B. Schumacher et al., Curr. Biol. 11 (21) (2001) 1722–1727.
[16] E.R. Hofmann et al., Curr. Biol. 12 (22) (2002) 1908–1918.
[17] S. Ito et al., Curr. Biol. 20 (4) (2010) 333–338.
[18] A. Sendoel et al., Nature 465 (7298) (2010) 577–583.
[19] C. Schertel, B. Conradt, Development 134 (20) (2007) 3691–3701.
[20] A.L. Craig et al., Methods Cell Biol. 107 (2012) 321–352.
[21] Y.C. Wu, X. Wang, D. Xue, Methods Cell Biol. 107 (2012) 295–320.

[22] J. Hodgkin, Introduction to genetics and genomics, in: T.C.e.R. Community, (Ed.), *WormBook*, 2005, pp. 1–3.
[23] B. Conradt, D. Xue, Programmed Cell Death, in: T.C.e.R. Community, (Ed.), WormBook, (2005) 1–13.
[24] H.R. Horvitz, ChemBioChem 4 (8) (2003) 697–711.
[25] F. Chen et al., Science 287 (5457) (2000) 1485–1489.
[26] D. Wu et al., J. Biol. Chem. 272 (34) (1997) 21449–21454.
[27] M.S. Spector et al., Nature 385 (6617) (1997) 653–656.
[28] E. Pourkarimi, S. Greiss, A. Gartner, Cell Death Differ. 19 (3) (2012) 406–415.
[29] X. Wang et al., Nat. Cell Biol. 9 (5) (2007) 541–549.
[30] X. Wang et al., Science 298 (5598) (2002) 1587–1592.
[31] R.C. Taylor et al., J. Biol. Chem. 282 (20) (2007) 15011–15021.
[32] E.D. Crawford et al., Cell Death Differ. 19 (12) (2012) 2040–2048.
[33] X. Wang et al., Science 302 (5650) (2003) 1563–1566.
[34] C. Grimsley, K.S. Ravichandran, Trends Cell Biol. 13 (12) (2003) 648–656.
[35] K.S. Ravichandran, Immunity 35 (4) (2011) 445–455.
[36] Z. Zhou, E. Hartwieg, H.R. Horvitz, Cell 104 (1) (2001) 43–56.
[37] J.M. Kinchen et al., Nat. Cell Biol. 10 (5) (2008) 556–566.
[38] J.M. Kinchen et al., Nature 434 (7029) (2005) 93–99.
[39] A.J. Ross et al., Cell Death Differ. 20 (4) (2011) 1140–1149.
[40] M. Dreze et al., Nat. Methods 6 (11) (2009) 843–849.
[41] E.A. Kritikou et al., Genes Dev. 20 (16) (2006) 2279–2292.
[42] C. Quevedo, D.R. Kaplan, W.B. Derry, Curr. Biol. 17 (3) (2007) 286–292.
[43] R. Rutkowski et al., PLoS Genet. 7 (8) (2011) e1002238.
[44] D.L. Church, K.L. Guan, E.J. Lambie, Development 121 (8) (1995) 2525–2535.
[45] A.J. Perrin et al., Cell Death Differ. 20 (1) (2013) 97–107.
[46] S. Greiss et al., Genes Dev. 22 (20) (2008) 2831–2842.
[47] Y. Gavrieli, Y. Sherman, S.A. Ben-Sasson, J. Cell Biol. 119 (3) (1992) 493–501.
[48] G. Lettre et al., Cell Death Differ. 11 (11) (2004) 1198–1203.
[49] L.J. Neukomm et al., Nat. Cell Biol. 13 (1) (2011) 79–86.
[50] X. Wang et al., Nat. Cell Biol. 12 (7) (2010) 655–664.
[51] A. Essex et al., Mol. Biol. Cell 20 (4) (2009) 1252–1267.
[52] R.A. Green et al., Cell 145 (3) (2011) 470–482.
[53] T. Stiernagle, Maintenance of *C. elegans*, in: T.C.E.R. (Ed.), Community, *WormBook*, 2005, 1–11.
[54] T. Sijen et al., Cell 107 (4) (2001) 465–476.
[55] M. Tijsterman et al., Curr. Biol. 12 (17) (2002) 1535–1540.
[56] C. Kumsta, M. Hansen, PLoS ONE 7 (5) (2012) e35428.
[57] S. Brenner, Genetics 77 (1974) 71–94.
[58] R.E. Ellis, D.M. Jacobson, H.R. Horvitz, Genetics 129 (1) (1991) 79–94.
[59] J. Yuan et al., Cell 75 (4) (1993) 641–652.
[60] J. Yuan, H.R. Horvitz, Development 116 (2) (1992) 309–320.
[61] M.O. Hengartner, R.E. Ellis, H.R. Horvitz, Nature 356 (6369) (1992) 494–499.
[62] W.B. Derry et al., Cell Death Differ. 14 (4) (2007) 662–670.
[63] D.M. Eisenmann, S.K. Kim, Genetics 146 (2) (1997) 553–565.
[64] X. Lu, H.R. Horvitz, Cell 95 (7) (1998) 981–991.
[65] M.R. Lackner, S.K. Kim, Genetics 150 (1) (1998) 103–117.